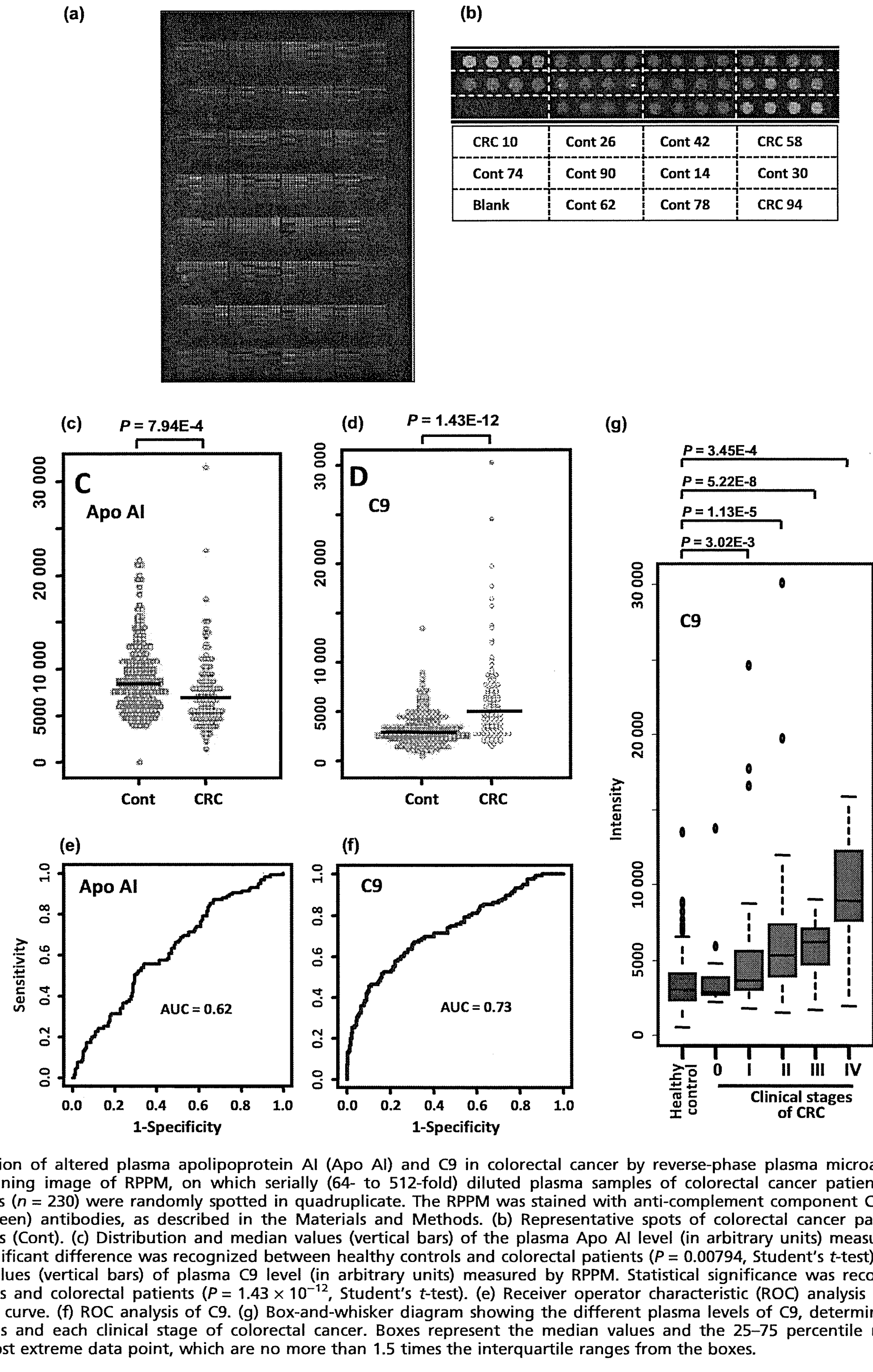

Fig. 3. Validation of altered plasma apolipoprotein AI (Apo AI) and C9 in colorectal cancer by reverse-phase plasma microarray (RPPM). (a) Dual-color scanning image of RPPM, on which serially (64- to 512-fold) diluted plasma samples of colorectal cancer patients (n = 115) and healthy controls (n = 230) were randomly spotted in quadruplicate. The RPPM was stained with anti-complement component C9 (red) and anti-human IgG (green) antibodies, as described in the Materials and Methods. (b) Representative spots of colorectal cancer patients (CRC) and healthy controls (Cont). (c) Distribution and median values (vertical bars) of the plasma Apo AI level (in arbitrary units) measured by RPPM. A statistically significant difference was recognized between healthy controls and colorectal patients (P = 0.00794, Student's t-test). (d) Distribution and median values (vertical bars) of plasma C9 level (in arbitrary units) measured by RPPM. Statistical significance was recognized between healthy controls and colorectal patients ($P = 1.43 \times 10^{-12}$, Student's t-test). (e) Receiver operator characteristic (ROC) analysis of Apo AI. AUC, area under the curve. (f) ROC analysis of C9. (g) Box-and-whisker diagram showing the different plasma levels of C9, determined by RPPM for healthy controls and each clinical stage of colorectal cancer. Boxes represent the median values and the 25–75 percentile ranges. Whiskers indicate the most extreme data point, which are no more than 1.5 times the interquartile ranges from the boxes.

(stages 0–II) and advanced (stages III and IV) colorectal cancer patients over healthy individuals were 0.594 and 0.810, respectively, indicating its inferiority to C9 in detecting early stage colorectal cancer.

Alterations of Apo AI and C9 in other cancers. Finally, we measured the level of Apo AI and C9 in 378 plasma samples collected prospectively from different medical institutions using RPPM. The observed alterations of plasma Apo AI and C9

Table 3. Alterations of plasma Apo AI and C9 in various diseases

	n	Apo AI			C9		
		Average†	SD	P value‡	Average†	SD	P value‡
Healthy control	109	4679.5	3265.6		527.2	674.7	
Colorectal cancer	100	2318.4	2015.0	1.71×10^{-9}	1792.7	1628.1	3.82×10^{-11}
Gastric cancer	105	2812.0	2357.5	3.00×10^{-6}	1629.6	1533.9	3.31×10^{-10}
Hepatocellular carcinoma	14	2621.6	2260.8	0.007	477.0	332.4	0.651
Esophageal cancer	10	3074.6	1572.6	0.014	1639.1	1036.7	0.008
Pancreatic cancer	14	2934.3	2214.8	0.016	1436.8	1125.6	0.010
Cholangiocarcinoma	18	1674.6	1377.0	1.26×10^{-8}	2519.6	2086.8	0.001
Pancreatitis	8	1925.9	1970.3	0.005	1564.4	1502.5	0.093

†Determined by RPPM (in arbitrary units). ‡Compared with healthy controls (student's t-test).

proteins in colorectal cancer patients were reproducible, even in this independent cohort (Table 3). The reduction of plasma Apo AI protein seems not to be specific to colorectal cancer, and was observed in patients with various cancers as well as chronic pancreatitis. The increment of plasma C9 protein was also not specific to colorectal cancer patients; patients with gastric cancer, esophageal cancer, pancreatic cancer and cholangiocarcinoma also showed a statistically significant increase of plasma C9 protein. The AUC value of C9 for colorectal cancer patients over healthy individuals (0.796) was higher than that of CEA (0.762; Fig. 4). The combination with C9 improved the AUC value of CEA from 0.762 to 0.852.

Discussion

The context of circulating blood proteins may represent underlying physiological and pathogenic conditions. Therefore, the blood proteome is considered an ample source of biomarker discovery. In order to identify a new biomarker that can be used for a non-invasive and inexpensive blood test of colorectal cancer, we first compared plasma proteome data using 2DICAL. We found that 10 proteins showed statistically significant differences between colorectal cancer patients and controls (Table 2). The differences of Apo AI and C9 were then verified by immunoblotting with relevant antibodies (Fig. 1c). Apo AI is the major protein component of plasma high density lipoprotein.[19] Apo AI has been repeatedly reported to be downregulated in the plasma samples of patients with various cancers including ovarian and pancreatic cancers.[20,21]

Any biomarker candidates identified by genomic or proteomic approaches must be validated in a statistically sufficient number of cases and controls using a different quantitative method before being considered for clinical application.[22,23] Accordingly, we determined the relative plasma levels of Apo AI and C9 in 345 individuals using RPPM (Fig. 3) and confirmed the results in an independent cohort consisting of 378 plasma samples collected from healthy controls and patients with various diseases (Table 3). The collection and storage of all the plasma samples were performed under the same protocol to exclude any sampling biases. Conventionally, ELISA has been used for such validation, but the standard sandwich ELISA assay requires two antibodies that do not interfere with each other. As a result, the development of ELISA usually takes several months for every biomarker candidate protein. And more importantly, ELISA requires a relative large volume (~100 μL) of samples. Because the supply of clinical materials is often limited, it may be unfavorable to use hundreds of microlitters of precise samples for preliminary experiments. Our high-density RPPM requires a minimal sample volume of the nanoliter order and one antibody. RPPM is an alternative validation method that can determine the

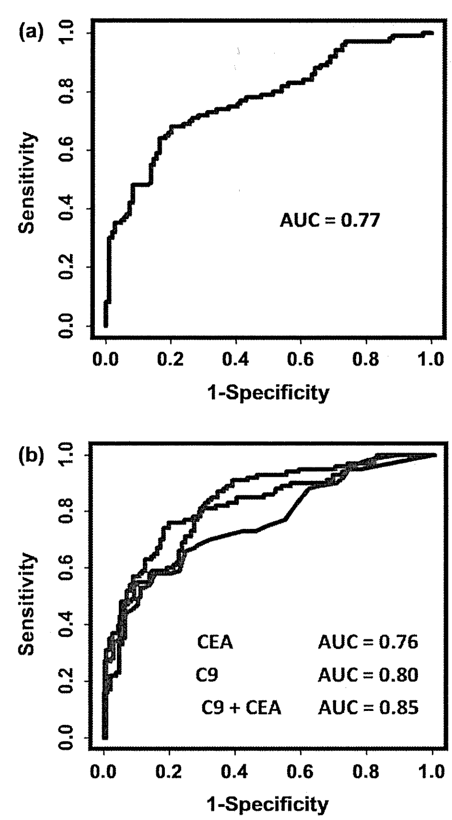

Fig. 4. Confirmation in an independent cohort. (a) Receiver operator characteristic (ROC) analysis of apolipoprotein AI (Apo AI; colorectal cancer patients [n = 100] over healthy controls [n = 109]). AUC, area under the curve. (b) ROC analysis of carcinoembryonic antigen (CEA), plasma complement component-9 (C9) and their combination (colorectal cancer patients [n = 100] over healthy controls [n = 109]).

clinical utility of candidate biomarker protein in a single experiment.[12]

Although protein microarray is a newly established technique and still requires improvement regarding validity and standardization,[24] it has been successfully used for analyzing clinical specimens of prostate cancer,[25] breast cancer,[26] rhabdomyosarcoma[27] and acute myeloid leukemia.[28,29] More recently, Grote *et al.*[30] used protein microarrays for the measurement of serum and plasma CA19-9. They printed a total of 149 sera and plasma samples obtained from pancreatic cancer patients, patients with chronic pancreatitis and healthy controls onto

doi: 10.1111/j.1349-7006.2010.01818.x

nitrocellulose-coated slide glasses and obtained results comparable to conventional ELISA. They used 200-μm pins, and signals were detected using diaminobenzidine as a chromogen. We were able to spot as many as 6144 protein samples into a glass slide using a 100-μm innovative screw-shaped pin and hydrophobic surface technologies. The hydrophobic surface of microarrays mediates tight interaction with proteins and prevents protein spot diffusion.[16,17] Only with all these cutting-edge technologies was this level of high-density spotting of adhesive protein samples possible. Fluorescence immunostaining of our RPPM provided wide dynamic range and high reproducibility (Fig. 2). The linearity of fluorescence intensity was obtained in a wide range, and over 78% of quadruplicate showed a CV of < 0.1 (Fig. 2c). All these make our RPPM a reliable tool for biomarker validation.

The ninth component of complement (C9) is one of five component proteins (C5b, C6, C7, C8 and C9) of the membrane attack complex (MAC).[31] The MAC attaches to the surface of target cells and forms a pore across the cell membrane resulting in complement-dependent cytotoxicity (CDC). Aberrant activation of MAC has been implicated in the pathogenesis of various autoimmune and infectious diseases. We previously identified the significant increase of complement components C3 and C4A in the sera of endometrial cancer patients.[9] In the present study we found the plasma level of C9 was significantly elevated in colorectal cancer patients, including those with stage I and II diseases. The expression of membrane-bound CD46, CD55 and CD59 protects cancer cells from CDC,[32] but the precise role of complements and these modifiers in the process of carcinogenesis has not been fully established. Further efforts will be necessary to clarify the biological significance of increased circulating C9 in patients with colorectal cancer.

In the present study we identified and validated C9 as a plasma biomarker potentially useful for the detection of early stage colorectal cancer using the combination of innovative proteomic technologies. Although the clinical significance of C9 must be clarified in an independent clinical study, we were able to demonstrate the utility of the combination of 2DICAL and RPPM in biomarker discovery and validation. The combination is a rapid approach that could be applicable to the discovery of biomarkers for any types of human malignancy.

Acknowledgments

The authors thank Mr M. Goto (Kakengeneqs, Matsudo) for engineering support for the protein microarrayer, Dr. Y. Sasakura, Mr S. Morikawa, Mr K. Kanda and Mr T. Mori (Hitachi HiTechnology, Tokyo) for helpful discussions about the ProteoChip, and Dr. S. Natsukawa (Saku Central Hospital, Saku), Dr. K. Shaura (Hokushin General Hospital, Nakano), Dr. Y. Koizumi (Shinonoi General Hospital, Nagano) and Dr. Y. Kasuga (Nagano Matsushiro General Hospital, Nagano) for the provision of clinical data. This work was supported by the Third-Term Comprehensive Control Research for Cancer and Research on Biological Markers for New Drug Development conducted by the Ministry of Health and Labor of Japan, and Program for Promotion of Fundamental Studies in Health Sciences conducted by the National Institute of Biomedical Innovation of Japan.

Disclosure Statement

No potential conflict of interest relevant to this paper is declared.

References

1 Parkin DM, Bray F, Ferlay J, Pisani P. Global cancer statistics, 2002. *CA Cancer J Clin* 2005; **55**: 74–108.
2 Okuno K. Surgical treatment for digestive cancer. Current issues – colon cancer. *Dig Surg* 2007; **24**: 108–14.
3 Wakai K, Hirose K, Matsuo K *et al.* Dietary risk factors for colon and rectal cancers: a comparative case–control study. *J Epidemiol* 2006; **16**: 125–35.
4 Duffy MJ, van Dalen A, Haglund C *et al.* Tumour markers in colorectal cancer: European Group on Tumour Markers (EGTM) guidelines for clinical use. *Eur J Cancer* 2007; **43**: 1348–60.
5 Liotta LA, Petricoin EF. Serum peptidome for cancer detection: spinning biologic trash into diagnostic gold. *J Clin Invest* 2006; **116**: 26–30.
6 Omenn GS, States DJ, Adamski M *et al.* Overview of the HUPO Plasma Proteome Project: results from the pilot phase with 35 collaborating laboratories and multiple analytical groups, generating a core dataset of 3020 proteins and a publicly-available database. *Proteomics* 2005; **5**: 3226–45.
7 Honda K, Hayashida Y, Umaki T *et al.* Possible detection of pancreatic cancer by plasma protein profiling. *Cancer Res* 2005; **65**: 10613–22.
8 States DJ, Omenn GS, Blackwell TW *et al.* Challenges in deriving high-confidence protein identifications from data gathered by a HUPO plasma proteome collaborative study. *Nat Biotechnol* 2006; **24**: 333–8.
9 Negishi A, Ono M, Handa Y *et al.* Large-scale quantitative clinical proteomics by label-free liquid chromatography and mass spectrometry. *Cancer Sci* 2009; **100**: 514–9.
10 Ono M, Shitashige M, Honda K *et al.* Label-free quantitative proteomics using large peptide data sets generated by nanoflow liquid chromatography and mass spectrometry. *Mol Cell Proteomics* 2006; **5**: 1338–47.
11 Matsubara J, Ono M, Negishi A *et al.* Identification of a predictive biomarker for hematologic toxicities of gemcitabine. *J Clin Oncol* 2009; **27**: 2261–8.
12 Matsubara J, Ono M, Honda K *et al.* Survival prediction for pancreatic cancer patients receiving gemcitabine treatment. *Mol Cell Proteomics* 2010; **9**: 695–704.
13 Machida-Montani A, Sasazuki S, Inoue M *et al.* Atrophic gastritis, *Helicobacter pylori*, and colorectal cancer risk: a case-control study. *Helicobacter* 2007; **12**: 328–32.
14 Ono M, Matsubara J, Honda K *et al.* Prolyl 4-hydroxylation of α-fibrinogen: a novel protein modification revealed by plasma proteomics. *J Biol Chem* 2009; **284**: 29041–9.
15 Honda K, Yamada T, Hayashida Y *et al.* Actinin-4 increases cell motility and promotes lymph node metastasis of colorectal cancer. *Gastroenterology* 2005; **128**: 51–62.
16 Lee Y, Lee EK, Cho YW *et al.* ProteoChip: a highly sensitive protein microarray prepared by a novel method of protein immobilization for application of protein–protein interaction studies. *Proteomics* 2003; **3**: 2289–304.
17 Sasakura Y, Kanda K, Yoshimura-Suzuki T *et al.* Protein microarray system for detecting protein–protein interactions using an anti-His-tag antibody and fluorescence scanning: effects of the heme redox state on protein-protein interactions of heme-regulated phosphodiesterase from *Escherichia coli*. *Anal Chem* 2004; **76**: 6521–7.
18 Greene FL. TNM staging for malignancies of the digestive tract: 2003 changes and beyond. *Semin Surg Oncol* 2003; **21**: 23–9.
19 Breslow JL, Ross D, McPherson J *et al.* Isolation and characterization of cDNA clones for human apolipoprotein A-I. *Proc Natl Acad Sci U S A* 1982; **79**: 6861–5.
20 Zhang Z, Bast RC Jr, Yu Y *et al.* Three biomarkers identified from serum proteomic analysis for the detection of early stage ovarian cancer. *Cancer Res* 2004; **64**: 5882–90.
21 Kozak KR, Su F, Whitelegge JP, Faull K, Reddy S, Farias-Eisner R. Characterization of serum biomarkers for detection of early stage ovarian cancer. *Proteomics* 2005; **5**: 4589–96.
22 Ransohoff DF. Rules of evidence for cancer molecular-marker discovery and validation. *Nat Rev Cancer* 2004; **4**: 309–14.
23 Ludwig JA, Weinstein JN. Biomarkers in cancer staging, prognosis and treatment selection. *Nat Rev Cancer* 2005; **5**: 845–56.
24 Wulfkuhle JD, Edmiston KH, Liotta LA, Petricoin EF 3rd. Technology insight: pharmacoproteomics for cancer – promises of patient-tailored medicine using protein microarrays. *Nat Clin Pract Oncol* 2006; **3**: 256–68.
25 Grubb RL, Calvert VS, Wulkuhle JD *et al.* Signal pathway profiling of prostate cancer using reverse phase protein arrays. *Proteomics* 2003; **3**: 2142–6.
26 Rapkiewicz A, Espina V, Zujewski JA *et al.* The needle in the haystack: application of breast fine-needle aspirate samples to quantitative protein microarray technology. *Cancer* 2007; **111**: 173–84.
27 Petricoin EF 3rd, Espina V, Araujo RP *et al.* Phosphoprotein pathway mapping: Akt/mammalian target of rapamycin activation is negatively associated with childhood rhabdomyosarcoma survival. *Cancer Res* 2007; **67**: 3431–40.

28 Tibes R, Qiu Y, Lu Y *et al.* Reverse phase protein array: validation of a novel proteomic technology and utility for analysis of primary leukemia specimens and hematopoietic stem cells. *Mol Cancer Ther* 2006; **5**: 2512–21.
29 Kornblau SM, Tibes R, Qiu YH *et al.* Functional proteomic profiling of AML predicts response and survival. *Blood* 2009; **113**: 154–64.
30 Grote T, Siwak DR, Fritsche HA *et al.* Validation of reverse phase protein array for practical screening of potential biomarkers in serum and plasma: accurate detection of CA19-9 levels in pancreatic cancer. *Proteomics* 2008; **8**: 3051–60.
31 Tschopp J, Podack ER, Muller-Eberhard HJ. Ultrastructure of the membrane attack complex of complement: detection of the tetramolecular C9-polymerizing complex C5b-8. *Proc Natl Acad Sci U S A* 1982; **79**: 7474–8.
32 Gorter A, Meri S. Immune evasion of tumor cells using membrane-bound complement regulatory proteins. *Immunol Today* 1999; **20**: 576–82.

Supporting Information

Additional Supporting Information may be found in the online version of this article:

Fig. S1. Verification of reverse-phase plasma microarray (RPPM).

Please note: Wiley-Blackwell are not responsible for the content or functionality of any supporting materials supplied by the authors. Any queries (other than missing material) should be directed to the corresponding author for the article.

doi: 10.1111/j.1349-7006.2010.01818.x

Supplementary Figure S1

(a)

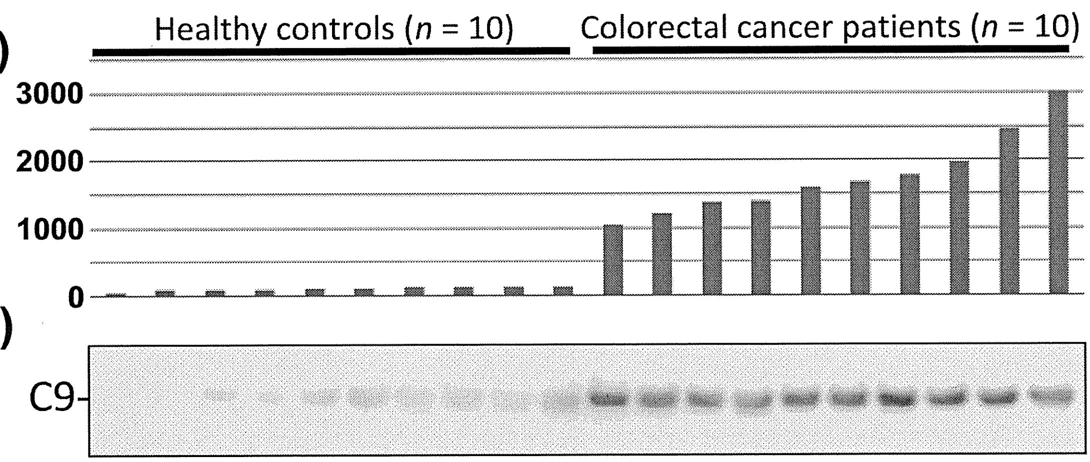

(b)

Supplementary Fig. S1.
Verification of reverse-phase plasma microarray (RPPM).
(a) Plasma complement component-9 (C9) level (in arbitrary unit) of 10 representative colorectal cancer patients and 10 healthy controls determined by RPPM.
(b) The same plasma samples were subjected to immunoblotting with anti-C9 antibody.

THE JOURNAL OF BIOLOGICAL CHEMISTRY VOL. 284, NO. 42, pp. 29041–29049, October 16, 2009

Prolyl 4-Hydroxylation of α-Fibrinogen

A NOVEL PROTEIN MODIFICATION REVEALED BY PLASMA PROTEOMICS*[S]

Received for publication, July 6, 2009, and in revised form, August 18, 2009 Published, JBC Papers in Press, August 20, 2009, DOI 10.1074/jbc.M109.041749

Masaya Ono,[a1] Junichi Matsubara,[a] Kazufumi Honda,[a] Tomohiro Sakuma,[b] Tomoyo Hashiguchi,[c] Hiroshi Nose,[c] Shoji Nakamori,[d] Takuji Okusaka,[e] Tomoo Kosuge,[f] Naohiro Sata,[g] Hideo Nagai,[g] Tatsuya Ioka,[h] Sachiko Tanaka,[h] Akihiko Tsuchida,[i] Tatsuya Aoki,[i] Masashi Shimahara,[j] Yohichi Yasunami,[k] Takao Itoi,[l] Fuminori Moriyasu,[l] Ayako Negishi,[a] Hideya Kuwabara,[b] Ayako Shoji,[b] Setsuo Hirohashi,[a] and Tesshi Yamada[a,l]

From the [a]Chemotherapy Division, National Cancer Center Research Institute, the [e]Pancreatic Oncology Division, and the [f]Hepatobiliary and Pancreatic Surgery Division, National Cancer Center Hospital, 5-1-1 Tsukiji, Chuo-ku, Tokyo 104-0045, the [b]Bioscience Team, Consulting Business Unit, Mitsui Knowledge Industry, 2-5-1 Atago, Minato-ku, Tokyo 105-6215, the [c]Kobe Research Center, Transgenic Inc., 7-1-14 Minatojimaminami-machi, Chuo-ku, Kobe 650-0047, the [d]Department of Surgery, Osaka National Hospital, 2-1-14 Hoenzaka, Chuo-ku, Osaka 540-0006, the [g]Department of Surgery, Jichi Medical School, 3311-1 Yakushiji, Minamikawachi, Tochigi 329-0498, the [h]Department of Hepatobiliary and Pancreatic Oncology, Osaka Medical Center for Cancer and Cardiovascular Diseases, 1-3-3 Nakamichi, Higashinari, Osaka 537-8511, the [i]Third Department of Surgery and [l]Fourth Department of Internal Medicine, Tokyo Medical University, 6-7-1 Nishi-Shinjuku, Shinjuku-ku, Tokyo 160-0023, the [j]Department of Oral Surgery, Osaka Medical College, 2-7 Daigaku-machi, Takatsuki-Shi, Osaka 569-8686, and the [k]Department of Regenerative Medicine and Transplantation, Fukuoka University Faculty of Medicine, 7-45-1 Nanakuma, Jonan-ku, Fukuoka 814-0180, Japan

Plasma proteome analysis requires sufficient power to compare numerous samples and detect changes in protein modification, because the protein content of human samples varies significantly among individuals, and many plasma proteins undergo changes in the bloodstream. A label-free proteomics platform developed in our laboratory, termed "Two-Dimensional Image Converted Analysis of Liquid chromatography and mass spectrometry (2DICAL)," is capable of these tasks. Here, we describe successful detection of novel prolyl hydroxylation of α-fibrinogen using 2DICAL, based on comparison of plasma samples of 38 pancreatic cancer patients and 39 healthy subjects. Using a newly generated monoclonal antibody 11A5, we confirmed the increase in prolyl-hydroxylated α-fibrinogen plasma levels and identified prolyl 4-hydroxylase A1 as a key enzyme for the modification. Competitive enzyme-linked immunosorbent assay of 685 blood samples revealed dynamic changes in prolyl-hydroxylated α-fibrinogen plasma level depending on clinical status. Prolyl-hydroxylated α-fibrinogen is presumably controlled by multiple biological mechanisms, which remain to be clarified in future studies.

For comprehensive analysis of plasma proteins, it is necessary to compare a sufficient number of blood samples to avoid simple interindividual heterogeneity, because the protein content of human samples varies significantly among individuals. Also, the provision of sufficient power is needed to detect protein modification because many plasma proteins undergo changes in the bloodstream (1). Even though the proteomic technologies have advanced (2, 3), there remains room for improvement. Different isotope labeling and identification-based methods have been developed for quantitative proteomics technologies (4–6), but the number of samples that can be compared by the current isotope-labeling methods is limited, and identification-based proteomics is unable to capture information regarding unknown modifications.

A label-free proteomics platform developed in our laboratory, termed "Two-Dimensional Image Converted Analysis of Liquid chromatography and mass spectrometry (2DICAL)[2] (7), simply compares the liquid chromatography and mass spectrometry (LC-MS) data and detects a protein modification by finding changes in the mass to charge ratio (m/z) and retention time (RT). Enhanced methods for accurate MS peak alignment across multiple LC runs have enabled the successful implementation of clinical studies requiring comparison of a large number of samples (8, 9). Using 2DICAL to analyze plasma samples of pancreatic cancer patients and healthy controls, novel prolyl hydroxylation of α-fibrinogen was successfully discovered.

Fibrinogen and its modification has been investigated because of its clinical importance (10, 11). On the other hand, prolyl hydroxylation has attracted attention after the discovery of the hypoxia-inducible factor 1α (HIF1α) prolyl-hydroxylase and its role in switching of HIF1α functions (12). Prolyl hydroxylation in other proteins has been energetically sought,

* This work was supported by the Program for Promotion of Fundamental Studies in Health Sciences conducted by the National Institute of Biomedical Innovation of Japan and by the Third-Term Comprehensive Control Research for Cancer conducted by the Ministry of Health, Labor and Welfare of Japan.

[S] The on-line version of this article (available at http://www.jbc.org) contains supplemental Figs. S1–S7 and Tables S1–S3.

[1] To whom correspondence should be addressed. Fax: 81-3-3547-5298; E-mail: masono@ncc.go.jp.

[2] The abbreviations used are: 2DICAL, two-dimensional image converted analysis of liquid chromatography and mass spectrometry; CC, correlation coefficient; Con A, concanavalin A; CV, coefficient of variance; ELISA, enzyme-linked immunosorbent assay; ESI, electrospray; αFG, fibrinogen α-chain; GANP, germinal center-associated nuclear protein; HIF1, hypoxia-inducible factor-1; HyP, hydroxyproline; MS, mass spectrometry; MS/MS, tandem mass spectrometry; m/z, mass-to-charge ratio; OPD, orthophenylenediamine; P4H, prolyl 4-hydroxylase; QTOF, quadrupole time-of-flight; RT, retention time; siRNA, small interfering RNA.

but only a few such proteins have been identified (13). Only one study has reported prolyl hydroxylation of fibrinogen at the β chain (14).

Here, we report the detection of prolyl 4-hydroxylated α-fibrinogen by plasma proteome analysis, a protein modification that dynamically changes in plasma depending on the clinical status and is a candidate plasma biomarker.

EXPERIMENTAL PROCEDURES

Clinical Samples—Seventy-seven plasma samples (38 patients with pancreatic ductal adenocarcinoma and 39 healthy controls) were obtained from the National Cancer Center Hospital (Tokyo, Japan) (Sets 1 and 2), and 9 plasma samples (5 patients with pancreatic ductal adenocarcinoma and 4 healthy controls) were obtained from the Tokyo Medical University Hospital (Tokyo, Japan) (Set 3) (15). 685 plasma samples from patients with various diseases and healthy controls (Sets 4) were collected prospectively from seven medical institutions associated with the "Third-Term Comprehensive Control Research for Cancer" and will be described in detail elsewhere.[3] Written informed consent was obtained from every subject. The study was reviewed and approved by the ethics committee of each institute.

Sample Preparation—To 20 μl of a plasma sample, 900 μl of phosphate-buffered saline and 100 μl of Con A-agarose (Vector, Burlingame, CA) were added, and the sample was incubated at 4 °C for 2 h. After extensive washing with phosphate-buffered saline, proteins bound to Con A were eluted by competition with 100 mM mannose. To 30 μl of the eluted sample, 10 μl of 5 M urea, 2.5 μl of 1 M NH_4HCO_3, and 3.3 μg of sequencing grade modified trypsin (Promega, Madison, WI) were added. After digestion at 37 °C for 20 h, peptides were dried with a SpeedVac concentrator (Thermo Electron, Holbrook, NY) and then dissolved in 50 μl of 0.1% formic acid.

LC-MS—LC-MS and data acquisition were performed as reported previously (7, 8). Briefly, the peptide samples were separated with a linear gradient from 0 to 80% acetonitrile in 0.1% formic acid at a flow rate of 200 nl/min for 60 min using the splitless nano-flow HPLC systems (DiNa (KYA, Tokyo, Japan)) (16). MS spectra were acquired every second in triplicate with nano-electrospray (nanoESI)-QTOF-MS (QTOF Ultima (Waters, Milford, MA)).

Peak Alignment Across Multiple LC-MS—MS peaks were detected, normalized, and quantified using the in-house 2DICAL software package, as described previously (7). To increase the accuracy of peak alignment across multiple LC-MS runs, we applied a greedy algorithm, which had been used for fast DNA sequence alignment, to supplement our previous method (8, 9).

Protein and Modification Identification—MS and MS/MS data were acquired by preparative LC-MS runs with a tolerance of ± 0.1 m/z and $\pm$ 0.5 min of RT using QTOF Ultima and linear ion trap (LTQ)-Orbitrap (Thermo Fisher Scientific, Waltham, MA) mass spectrometers. The MS/MS data were analyzed with Mascot software (Matrix Sciences, London, UK) including oxidized histidine, oxidized methionine, and hydroxyproline as possible modifications. Chemical formulas were determined with Xcalibur software (Thermo Fisher Scientific) with mass tolerance of 5 ppm.

Cell Lines—Primary cultured normal hepatic cells (hNHeps) were purchased from Takara Bio (Shiga, Japan). KIM-1 was kindly provided by Dr. Masamichi Kojiro (Kurume University, Kurume, Japan). Hep3B was obtained from the Cell Resource Center for Biomedical Research, Tohoku University (Sendai, Japan). HLE was obtained from the Health Science Research Resources Bank (Osaka, Japan). SK-Hep-1, Jhh-7, Hep-G2, HuH-7, and HuH-6clone5 were purchased from the American Type Culture Collection (ATCC, Manassas, VA).

RNA Interference—Three siRNAs targeting each of the *P4HA1*, *P4HA2*, *P4HA3*, *P4HB*, *EGNL1*, *EGNL2*, and *EGNL3* genes, as well as 2 control RNAs, were designed by Applied Biosystems (Foster City, CA). Cells were transfected with the Lipofectamine 2000 reagent (Invitrogen, Carlsbad, CA) (17). Knockdown of relevant mRNA expression was confirmed by real-time PCR at 24 h after transfection (16).

Antibodies—Anti-fibrinogen antibody (A0080) was purchased from DAKO (Glostrup, Denmark). GANP transgenic mice (18) were immunized with a synthetic peptide ESSSHHP-(O)GIAEFPSR (P(O), hydroxyproline) (named HyP-ESS) conjugated to keyhole limpet hemocyanin. Monoclonal antibodies were generated by a standard cell fusion technique. The reactivity and titer of antibodies to HyP-ESS as well as unmodified (ESS) peptides were assessed by an antibody capture assay (19) using OPD (orthophenylenediamine) as a substrate (supplemental Fig. S6*A*).

Immunoblotting—Protein samples were separated by SDS-PAGE and electroblotted onto polyvinylidene difluoride membranes (Millipore, Billerica, MA). Blots were visualized with an enhanced chemiluminescence kit (GE Healthcare, Bucks, UK) and quantified as described previously (20).

Competitive ELISA—100 μl of plasma diluted 20-fold with phosphate-buffered saline or 100 μl of serially diluted HyP-ESS standard peptide were incubated with 100 μl of 1 μg/ml horseradish peroxidase-conjugated 11A5 antibody for 30 min. 50 μl of the solution was added to 96-well microtiter plates precoated with 50 ng of HyP-ESS peptide and incubated for 1 h. After extensive washing, wells were incubating with the OPD solution for 10 min, and color absorbance at 490 nm was measured (supplemental Fig. S6*D*).

Statistical Analyses—Mann-Whitney *U* test was performed with the open-source statistical language R (version 2.7.0) (9).

RESULTS

Large Scale Quantitative Plasma Proteomics of Pancreatic Cancer Patients—77 plasma samples (39 from patients with pancreatic cancer and 38 from healthy controls) were obtained from National Cancer Center Hospital. We used concanavalin A (Con A) to concentrate plasma glycoproteins (21). This "glycocapturing" procedure removed albumin and reduced the concentration of other abundant plasma proteins (22). Various aberrations of protein glycosylation accumulate in cancer (23,

[3] K. Honda, T. Okusaka, K. Felix, T. Umaki, M. Ono, S. Nakamori, N. Sata, H. Nagai, T. Ioka, S. Tanaka, A. Tsuchida, T. Aoki, T. Shimahara, M. Shimahara, Y. Yasunami, H. Kuwabara, Y. Otsuka, N. Ota, C. Ebihara, T. Kosuge, S. Hirohashi, M. W. Büchler, and T. Yamada, manuscript in preparation.

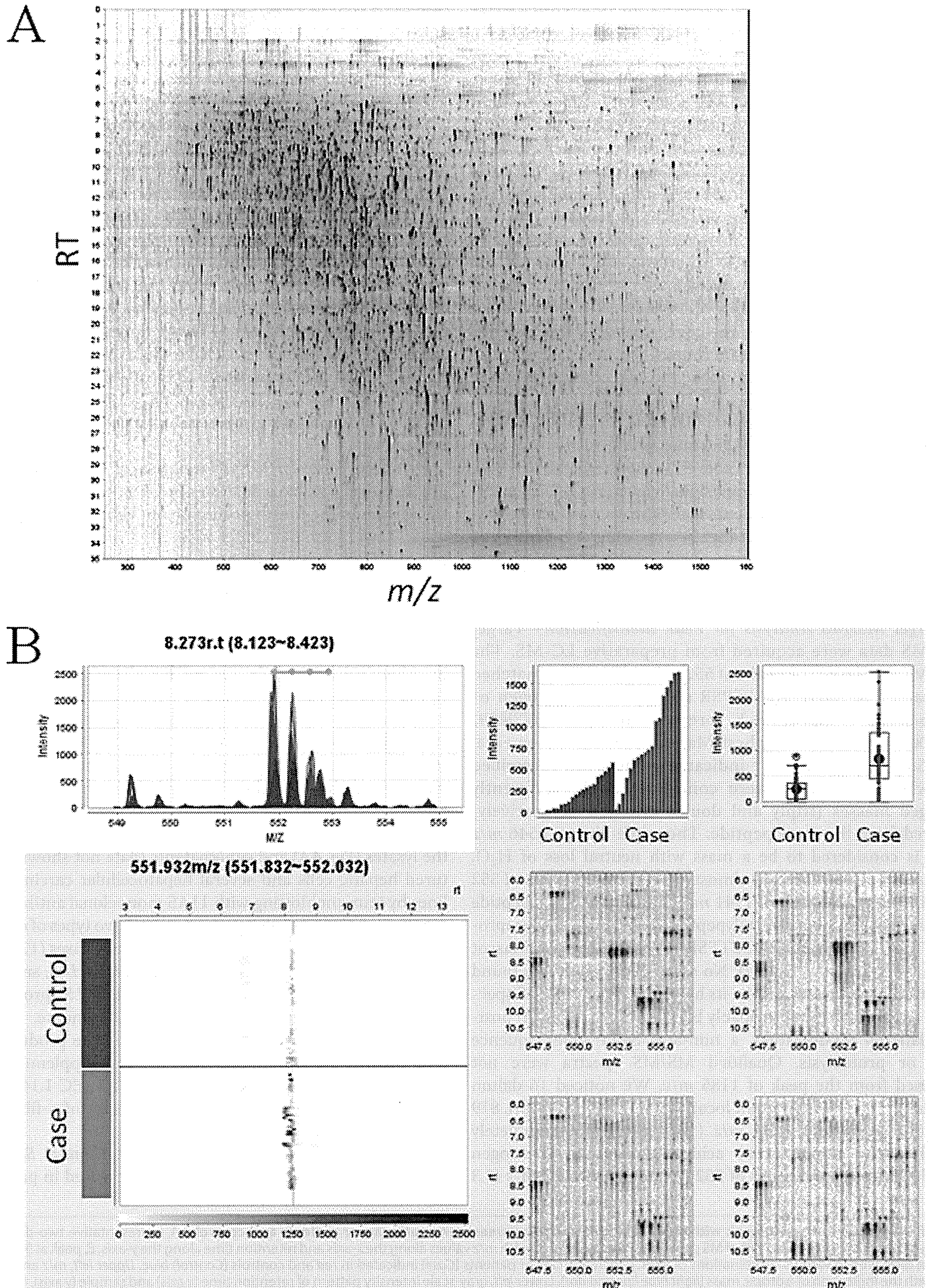
A
RT
m/z
B
8.273r.t (8.123~8.423)
Intensity
M/Z
551.932m/z (551.832~552.032)
Control
Case
Control Case
Control Case
rt
m/z

24). Most tumor markers of pancreatic cancer used clinically, including CA19-9, DUPAN-2, and NCC-ST-439, are known to be carbohydrate antigens (23, 25). Each sample was anonymized, randomized, and measured in triplicate by 2DICAL. A total of 115,325 independent MS peaks were detected within mass ranges of 250–1600 *m/z* and an LC RT of 0–45 min (Fig. 1*A*). The correlation coefficient (CC) and coefficient of variance (CV) values for the triplicate data were over 0.95 and under 0.15, respectively, in most subjects. To increase statistical robustness, 77 samples were separated at random into two experimental sets (Set 1 (18 pancreatic cancer patients and 19 healthy controls) and Set 2 (20 pancreatic cancer patients and 20 healthy controls)), and the two sets were analyzed independently. We selected 10 peptide peaks showing a statistically significant difference between the cancer patients and controls (>2 fold difference, $p < 0.0005$ (Mann-Whitney *U* test), average peak intensity of >10 in either the cancer samples or the control samples) in both sets. We further selected 6 peaks of 412 *m/z* (RT 13.7 min), 546 *m/z* (8.3 min), 552 *m/z* (8.3 min), 827 *m/z* (8.3 min), 1141 *m/z* (29.0 min), and 1185 *m/z* (9.2 min) (supplemental Fig. S1 and Table S1) inspecting the 2DICAL reports with various two-dimensional views (Fig. 1*B*). The difference between cancer patients and controls was further validated in an independent set (Set 3, consisting of 5 pancreatic cancer patients and 4 healthy controls) obtained from another medical institution (Tokyo Medical University Hospital) (supplemental Fig. S2).

Target MS/MS Analysis for Peak Identification—Target MS/MS data were acquired from preparative LC-MS. The MS/MS spectra of the peaks of 552 *m/z* and 827 *m/z* matched the same ESSSHHP*GIAEFPSR sequence of fibrinogen α-polypeptide isoform α-E preproprotein (NP_000499/NP_068657) with the highest Mascot scores (supplemental Fig. S3 and not shown; * indicates a mismatch (described below)). These peaks were considered to be differently charged masses (triply and doubly charged, respectively) derived from the same peptide. The triple-charged 546 *m/z* peak is considered to be a mass with neutral loss of H_2O, because its appearance was almost identical to the peaks of 552 and 827 *m/z*. The peak of 1141 *m/z* matched another peptide sequence of fibrinogen α-polypeptide isoform α-E preproprotein TFP*GFFSPMLGEFVSETESR with the highest Mascot score (supplemental Fig. S4). No significant match was found with the 412 *m/z* peak despite its highly qualified MS/MS spectrum (data not shown), probably because of an unknown post-translational modification, a non-annotated gene sequence (26), or proteolysis. Qualified MS/MS spectra were not obtained from the peak of 1185 *m/z*. We noticed 16-dalton smaller MS peaks at different locations (547 *m/z* (8.5 min), 819 *m/z* (8.6 min), and 1133 *m/z* (30.0 min)) that completely matched the same amino acid sequences of fibrinogen α-polypeptide as the peaks of 552 *m/z* (8.3 min), 827 *m/z* (8.3 min), and 1141 *m/z* (29.0 min), respectively (Fig. 2 and data not shown). However, the intensity of the three 16-dalton-smaller MS peaks did not differ significantly between pancreatic cancer patients and controls (Fig. 2*B*).

Determination of the 16-Dalton Increase by High Resolution MS—To clarify the nature of the 16-dalton increase, the peptides of 827 and 819 *m/z* as well as 1141 and 1133 *m/z* were analyzed with a high resolution Orbitrap mass spectrometer. The difference between both the larger and the smaller pairs was 15.995 dalton, considered to be derived exclusively from the addition of one oxygen atom (Fig. 3, *A* and *B*). MS/MS revealed that the addition took place on the proline 565 and 530 residues (Fig. 3*C* and supplemental Fig. S5*A*). A 155.0808 *m/z* fragment observed in the high resolution MS/MS spectrum of the 819 *m/z* peak and a 171.0762 *m/z* fragment observed in the spectrum of the 827 *m/z* peak led to the exclusive identification of their chemical formulas as $C_7H_{11}O_2N_2$ and $C_7H_{11}O_3N_2$, respectively (Fig. 3*D*). Formulas $C_7H_{11}O_3N_2$ and $C_7H_{11}O_2N_2$ match hydroxyproline-glycine and unmodified proline-glycine, respectively.

Detection of Prolyl 4-Hydroxylation of α-Fibrinogen—The physiologically stable oxidation of proline occurs exclusively at the carbon in the fourth position (supplemental Fig. S5*B*). We used *Ganp* (germinal center-associated nuclear protein) (27) transgenic mice to produce a monoclonal antibody (named 11A5) that reacts with a synthetic peptide ESSSHHP(O)-GIAEFPSR (P(O), 4-hydroxyproline) (named HyP-ESS) but not with an unmodified synthetic peptide with the same amino acid sequence (ESS) (supplemental Fig. S6*A*). GANP mice can produce highly diverse antibodies and have been used with success to generate high affinity antibodies to various difficult antigens (18). We were unable to produce a monoclonal antibody with specificity for TFP(O)GFFSPMLGEFVSETESR (data not shown). Fibrinogen α-polypeptide is produced and secreted mainly by the liver. α-Fibrinogen with hydroxylation of its proline 565 residue (hereafter, αFG-565HyP) as well as 3 polypeptides (the α-, β-, and γ-chains) of fibrinogen were detected in the lysates (Fig. 4*A*) and supernatants (data not shown) of cultured hepatic cells and several hepatocellular carcinoma cell lines by immunoblotting with 11A5 monoclonal antibody. The 4-hydroxylation of proline is catalyzed by two types of enzymes: collagen-type and HIF1-type prolyl 4-hydroxylases (12, 28, 29). There are 4 collagen-type (*P4HA1*, *P4HA2*, *P4HA3*, and *P4HB*) and 3 HIF1-type (*EGNL1*, *EGNL2*, and *EGNL3*) prolyl 4-hydroxylase genes annotated in the human genome, but only knockdown of *P4HA1* by siRNA inhibited the production of αFG-565HyP by KIM-1 cells (Fig. 4*B* and supplemental Fig. S7A), indicating the involvement of P4HA1 (EC 1.14.11.2) in the 4-hydroxylation of the proline 565 residue of α-fibrinogen, at least in this cell line.

Prolyl 4-Hydroxylated α-Fibrinogen in Clinical Samples—The plasma level of αFG-565HyP was increased in pancreatic

FIGURE 1. **Representative MS peak with significant difference between pancreatic cancer patients and controls.** *A*, representative two-dimensional display of the entire set (>110,000) of MS peaks detected by 2DICAL with *m/z* values along the *x*-axis and retention time along the *y*-axis. *B*, peak at 552 *m/z* and 8.3 min displayed in various combinations of axes. Pancreatic cancer patients (*Case*) indicated in *red* and controls (*Control*) *blue*. *Upper left*, *m/z* and intensity axes with the indication of isotopic mass (*light blue line* and *dot*). *Lower left*, gray-scale intensity pattern of retention time (*x* axis) and sample (*y* axis). *Upper right*, sample and intensity axes (*left*) and a *box-and-whisker diagram* of pancreatic cancer patients and controls (*right*). *Lower right*, *m/z* and retention time axes with high (*upper*) and low (*lower*) intensities indicated by a *red dot*.

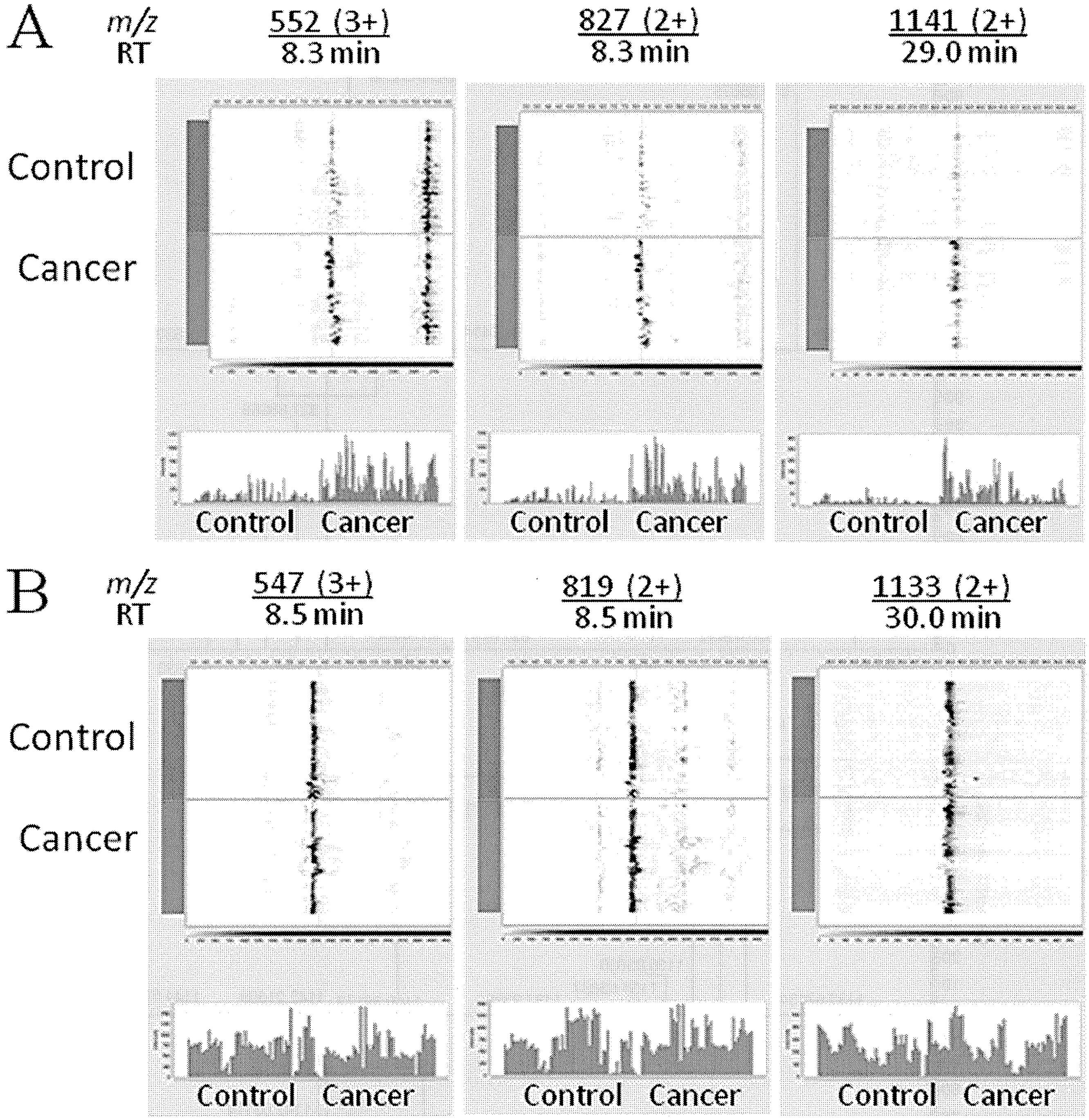

FIGURE 2. **Modified and unmodified peptide fragments with the same amino acid sequences.** *A*, peaks at 552, 827, 1141 *m/z* with significant difference between pancreatic cancer patients and controls. The axes are retention time and sample (*top*) and sample and intensity (*bottom*). *B*, peaks at 547, 819, and 1133 *m/z* matched to the above peaks of peptide fragment without modification.

cancer patients, but the levels of α-, β-, and γ-fibrinogen did not show any differences between pancreatic cancer patients and healthy controls (Fig. 4*C*). The levels of αFG-565HyP and α-fibrinogen were not significantly correlated (CC = 0.22) (supplemental Fig. S6, *B* and *C*). There was a significant correlation (CC = 0.81) between the intensity of the 827 *m/z* peak detected by 2DICAL and the level of αFG-565HyP determined by immunoblotting with 11A5 antibody (supplemental Fig. S7*B*), indicating the quantitative accuracy of 2DICAL. A competitive ELISA utilizing anti-HyP-ESS (11A5) monoclonal antibody was constructed (supplemental Fig. S6*D*), and the plasma level of αFG-565HyP was quantified in 685 individuals (Set 4) (Fig. 5). The plasma samples were collected prospectively from 7 medical institutions to ensure the absence of bias during the process of sample preparation. The ELISA assay showed high reproducibility with a median CV value of 0.079 among triplicates. There was a significant difference ($p = 3.80 \times 10^{-15}$, Mann-Whitney *U* test) in the plasma level of αFG-565HyP between 160 pan-

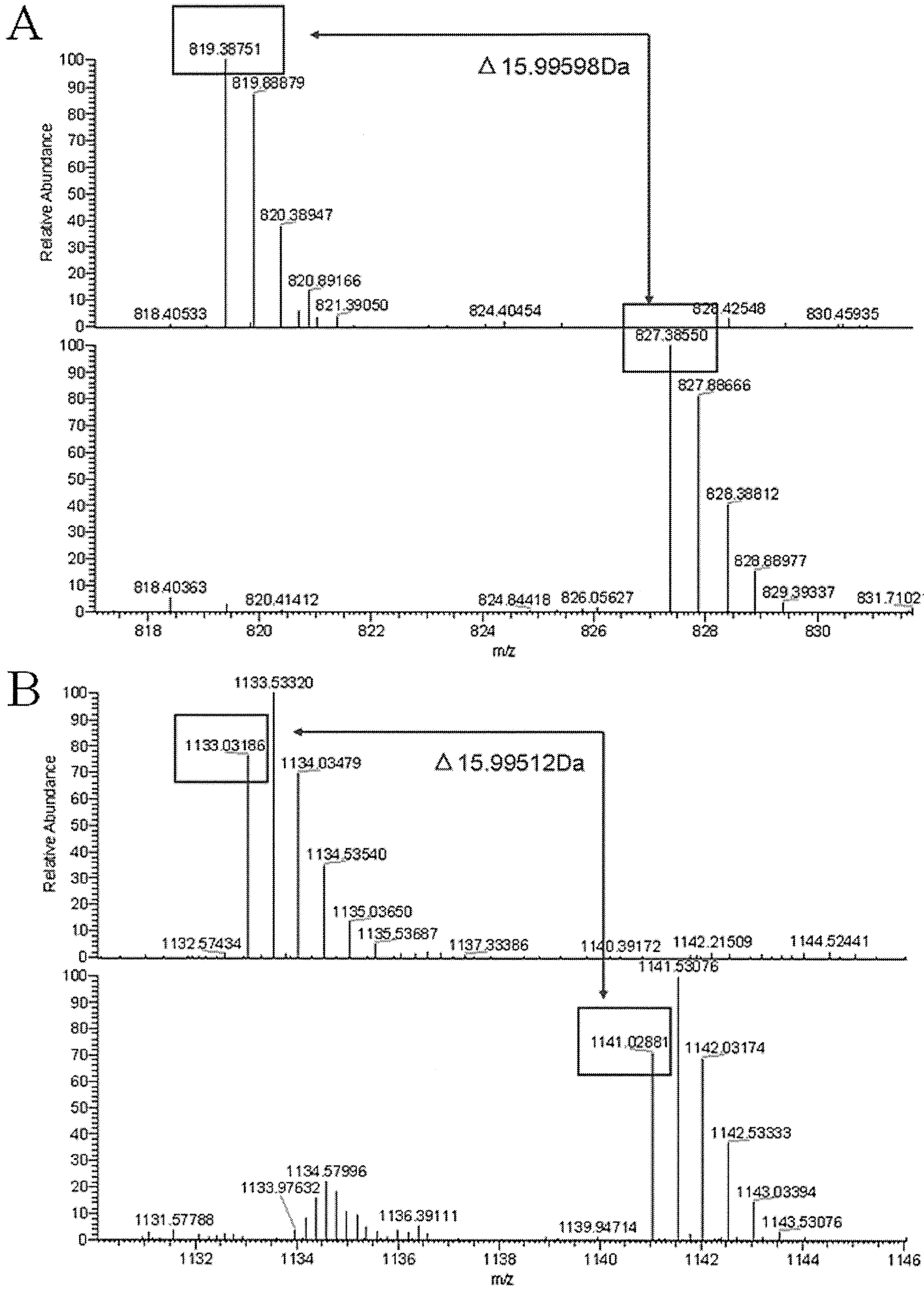

FIGURE 3. **Determination of the 16-dalton increase by high resolution MS.** *A* and *B*, high resolution MS spectra of the 827 and 819 *m/z* peaks (*A*) as well as the 1141 and 1133 *m/z* peaks (*B*) obtained with an Orbitrap mass spectrometer. *C*, MS/MS spectra of the 827, 1141, 819, and 1133 *m/z* peaks. *D*, 155.0808 *m/z* and 171.0762 *m/z* fragments exclusively identified as $C_7H_{11}O_2N_2$ and $C_7H_{11}O_3N_2$ with 5 ppm mass tolerance.

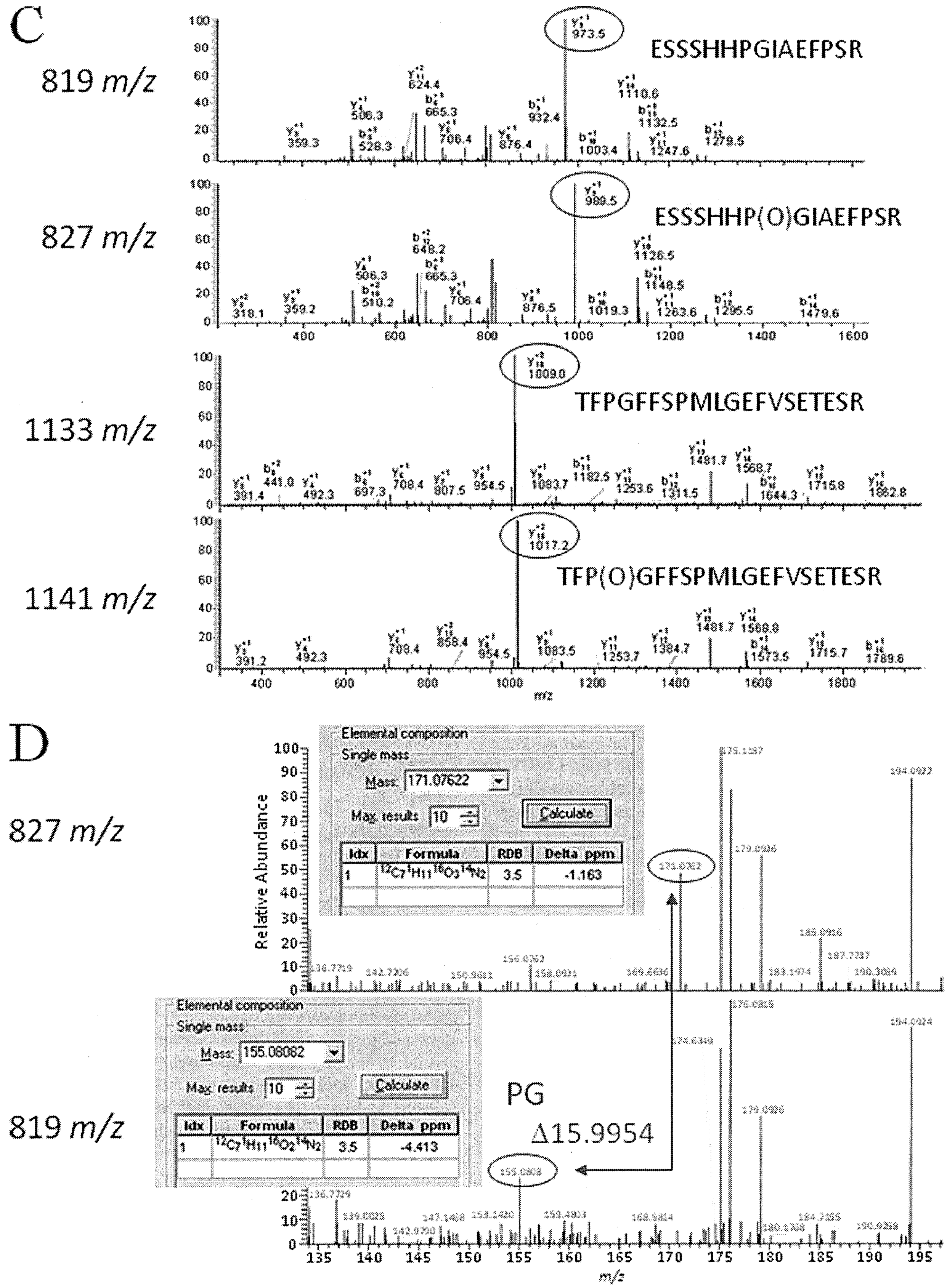

FIGURE 3—*continued*

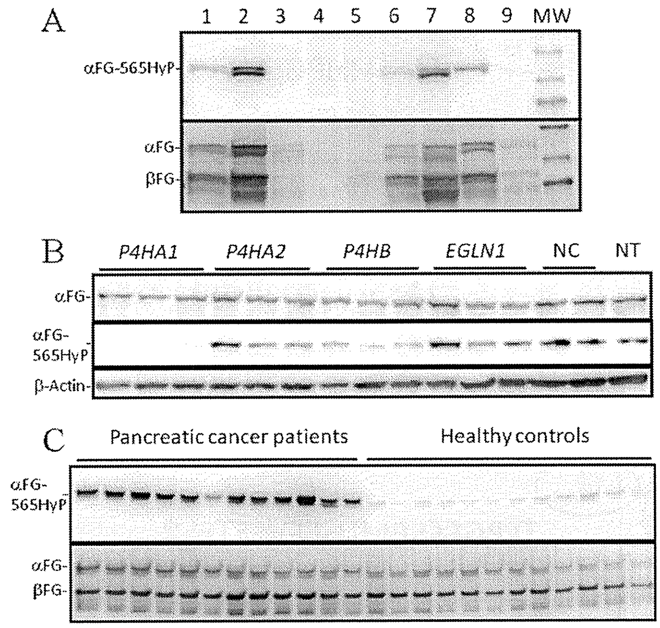

FIGURE 4. **Detection of prolyl 4-hydroxylated α-fibrinogen by immunoblotting.** *A*, lysates of normal hepatic cells (*lane 1*) and hepatocellular carcinoma KIM-1 (*lane 2*), Hep-3B (*lane 3*), SK-Hep-1 (*lane 4*), HLE (*lane 5*), Jhh-7 (*lane 6*), Hep-G2 (*lane 7*), HuH-7 (*lane 8*), and HuH-6clone5 (*lane 9*) cells were separated by SDS-PAGE and immunoblotted with anti-HyP-ESS and anti-fibrinogen (*FG*) antibodies. *B*, expression of the indicated genes was knocked in KIM-1 cells down by siRNA treatment (3 siRNAs for each gene). Forty-eight hours after transfection, the cell lysates were analyzed by immunoblotting with anti-HyP-ESS, anti-fibrinogen, and anti-β-actin (loading control) antibodies. *NC*, negative control (non-targeting RNA); *NT*, not treated. *C*, immunoblot analysis of plasma samples from pancreatic cancer patients and controls with anti-HyP-ESS and anti-fibrinogen antibodies.

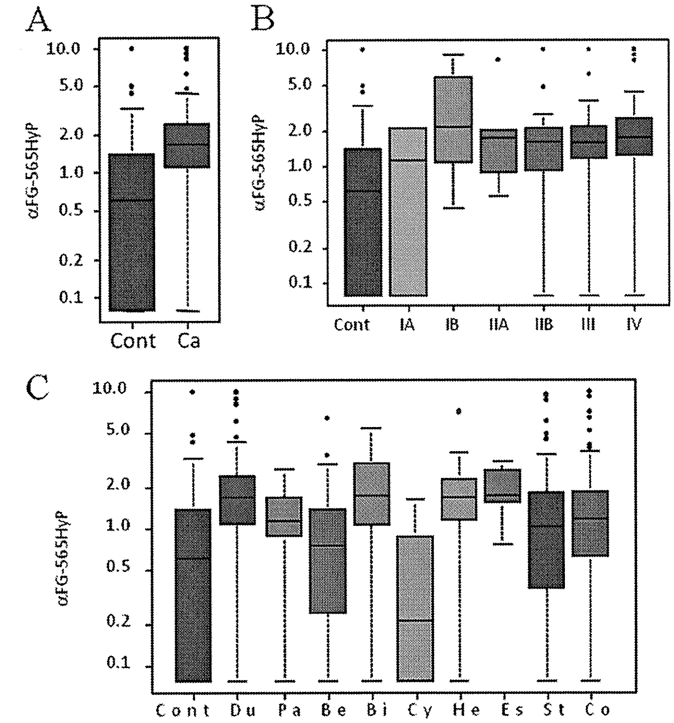

FIGURE 5. **Quantification of plasma prolyl 4-hydroxylated α-fibrinogen.** *A*, *box-and-whisker diagram* showing the different plasma levels of αFG-565Hyp in healthy controls (*Cont*, $n = 113$) and pancreatic cancer patients (*Ca*, $n = 160$). *Boxes* represent the median values and the 25–75 percentile range. *Whiskers* indicate the most extreme data point, which is no more than 1.5 times the interquartile range from the *boxes*. *B*, *box-and-whisker diagram* showing the plasma level of αFG-565Hyp in healthy controls (*Cont*, $n = 113$) and patients with stage-IA ($n = 2$), IB ($n = 4$), IIA ($n = 5$), IIB ($n = 28$), III ($n = 41$), and IV ($n = 78$) pancreatic cancer. *C*, *box-and-whisker diagram* showing the plasma level of αFG-565Hyp in healthy controls (*Cont*, $n = 113$) and patients with pancreatic ductal carcinoma (*Du*, $n = 160$), chronic pancreatitis (*Pa*, $n = 12$), benign pancreatic tumor or cyst (*Be*, $n = 37$), bile duct cancer (*Bi*, $n = 25$), cholecystitis (*Cy*, $n = 22$), hepatocellular carcinoma (*He*, $n = 14$), esophageal cancer (*Es*, $n = 10$), gastric cancer (*St*, $n = 147$), and colorectal cancer (*Co*, $n = 145$).

creatic cancer patients (2.26 ± 2.28 arbitrary units) and 113 healthy controls (0.91 ± 1.24) (Fig. 5*A*). The plasma level of αFG-565HyP was not elevated in patients with Stage IA (UICC, International Union Against Cancer) pancreatic cancer ($p = 0.811$), but patients with Stage IB or more advanced disease showed a significant increase of plasma αFG-565HyP ($p = 2.99 \times 10^{-2}$ to 1.88×10^{-12}) (Fig. 5*B* and supplemental Table S2). An elevated plasma level of αFG-565HyP was also observed in various cancers and chronic inflammatory disease. Patients with cancers of other organs (including the bile duct ($p = 4.24 \times 10^{-5}$), liver ($p = 1.08 \times 10^{-3}$), esophagus ($p = 2.07 \times 10^{-4}$), stomach ($p = 5.95 \times 10^{-4}$), and colon/rectum ($p = 9.29 \times 10^{-6}$)) as well as patients with chronic pancreatitis ($p = 3.89 \times 10^{-2}$) showed a significant increase in plasma αFG-565HyP (Fig. 5*C* and supplemental Table S3). Patients with benign pancreatic tumor/cyst ($p = 0.216$) or cholecystitis ($p = 0.111$) showed no significant difference from the controls.

DISCUSSION

Plasma proteomics by liquid chromatography and mass spectrometry (LC-MS) has been a challenge because of the complexity and individual diversity of human samples. We developed a simple but robust method that enables the quantitative comparison of multiple LC-MS data. In this study, we identified 6 MS peaks whose intensity was significantly different between 38 cancer patients and 39 healthy controls (Figs. 1 and 2 and supplemental Figs. S1 and S2) among a total of 115,325 peaks derived from Con A-binding plasma glycoproteins. High resolution MS/MS analysis revealed that 4 of 6 peaks were derived from prolyl 4-hydroxylated plasma α-fibrinogen (Fig. 3). Artificial oxidation of peptides/proteins frequently occurs during the preparative procedures for MS analysis, especially during separation by SDS-PAGE. However, the plasma samples from cancer patients and healthy controls used in this study were collected, stored, and processed in an identical manner and were not separated by SDS-PAGE. We deliberately validated the native hydroxylation of the proline residue of plasma α-fibrinogen by immunoblotting and ELISA with a modification-specific monoclonal antibody (Figs. 4 and 5).

Prolyl hydroxylation is essential for the folding, secretion, and stability of the collagen triple helix (28, 29). Collagen has long been considered to be the only protein that is hydroxylated on its proline residues, but recently the von Hippel Lindau (VHL) tumor suppressor gene product-mediated degradation of HIF1α was revealed to be regulated by prolyl hydroxylation (12). Prolyl 4-hydroxylation regulates the stability of argonaute 2 protein (13). However, it is largely unknown which other proteins are prolyl-hydroxylated and how the modification regulates the function of proteins. We found that the collagen-type prolyl 4-hydroxylase P4HA1 is essential for the production of αFG-565HyP (Fig. 4*B*). Consistently, the consensus Xaa-Pro-Gly sequence of collagen (13, 30) was seen in the prolyl hydroxylation sites of α-fibrinogen (supplemental Fig. S5*A*). Prolyl-hydroxylated α-fibrinogen was produced in cultured hepatic cells and several hepatocellular carcinoma cell lines but not in pancreatic cancer cell lines (data not shown). Immunohistochemical study using antibody 11A5 showed that prolyl-hydroxylated α-fibrinogen existed at the inflammation site around the pancreatic cancer cells (data not shown). The modification change in plasma level may be determined by the production and consumption balance in the human body. Hydroxylation at proline 530 of α-fibrinogen was strongly correlated with αFG-565HyP (supplementary Fig. S7*C*). Multiple biological mechanisms may be involved in the regulation of prolyl-hydroxylated α-fibrinogen.

Post-translational modifications, such as glycosylation, phosphorylation, and oxidation, cause small differences in the molecular weight of proteins. Prolyl-hydroxylated peptides are 16 daltons larger than their unmodified counterparts, but this small change in molecular weight can readily be detected by 2DICAL as differences in the m/z values as well as the RT of the peptide peaks. The peaks derived from unmodified plasma fibrinogen fragments appeared in different locations (compare Fig. 2, *A* and *B*). Such modifications may be overlooked by MS/MS-based identification-oriented proteome approaches (31–34).

In this study, we were able to pinpoint the prolyl 4-hydroxylation of α-fibrinogen peptides in the large dataset of plasma samples (115,325 MS peaks × 231 LC-MS runs (77 cases in triplicate) = 27 million data points). Using a large independent validation cohort, newly constructed ELISA assay revealed the plasma level elevation of prolyl 4-hydroxylated α-fibrinogen in pancreatic cancer as well as other cancers and chronic inflammatory disease. Future studies will reveal the function of prolyl-hydroxylated α-fibrinogen and its regulation and clinical usage.

Acknowledgments—We thank Dr. Toshiaki Isobe, Dr. Hiroyuki Kaji (Tokyo Metropolitan University, Tokyo, Japan), and Dr. Hiroshi Nakayama (The Institute of Physical and Chemical Research (RIKEN), Wako, Japan) for suggestions on the interpretation of MS/MS data and Dr. Tomikazu Sasaki (University of Washington, Seattle, WA) for suggestions on prolyl hydroxylation. We also thank Dr. Masamichi Kojiro (Kurume University, Kurume, Japan) for provision of KIM-1 cells. We thank Ayako Igarashi, Tomoko Umaki, and Yuka Nakamura for excellent technical assistance and Daisuke Higo (Thermofisher Scientific, Tokyo, Japan) for Orbitrap mass spectrometry.

REFERENCES

1. Nedelkov, D., Kiernan, U. A., Niederkofler, E. E., Tubbs, K. A., and Nelson, R. W. (2005) *Proc. Natl. Acad. Sci. U.S.A.* **102,** 10852–10857
2. Ishihama, Y. (2005) *J. Chromatogr. A.* **1067,** 73–83
3. Takahashi, N., Kaji, H., Yanagida, M., Hayano, T., and Isobe, T. (2003) *J. Nutr.* **133,** 2090S–2096S
4. Gygi, S. P., Rist, B., Gerber, S. A., Turecek, F., Gelb, M. H., and Aebersold, R. (1999) *Nat. Biotechnol.* **17,** 994–999
5. DeSouza, L., Diehl, G., Rodrigues, M. J., Guo, J., Romaschin, A. D., Colgan, T. J., and Siu, K. W. (2005) *J. Proteome. Res,* **4,** 377–386
6. Ong, S. E., Blagoev, B., Kratchmarova, I., Kristensen, D. B., Steen, H., Pandey, A., and Mann, M. (2002) *Mol. Cell Proteomics* **1,** 376–386
7. Ono, M., Shitashige, M., Honda, K., Isobe, T., Kuwabara, H., Matsuzuki, H., Hirohashi, S., and Yamada, T. (2006) *Mol. Cell Proteomics* **5,** 1338–1347
8. Negishi, A., Ono, M., Handa, Y., Kato, H., Yamashita, K., Honda, K., Shitashige, M., Satow, R., Sakuma, T., Kuwabara, H., Omura, K., Hirohashi, S., and Yamada, T. (2009) *Cancer Sci.* **100,** 514–519
9. Matsubara, J., Ono, M., Negishi, A., Ueno, H., Okusaka, T., Furuse, J., Furuta, K., Sugiyama, E., Saito, Y., Kaniwa, N., Sawada, J., Honda, K., Sakuma, T., Chiba, T., Saijo, N., Hirohashi, S., and Yamada, T. (2009) *J. Clin. Oncol.* **27,** 2261–2268
10. Blombäck, B. (2001) *Ann. N. Y. Acad. Sci.* **936,** 1–10
11. Henschen-Edman, A. H. (2001) *Ann. N. Y. Acad. Sci.* **936,** 580–593
12. Jaakkola, P., Mole, D. R., Tian, Y. M., Wilson, M. I., Gielbert, J., Gaskell, S. J., Kriegsheim, Av., Hebestreit, H. F., Mukherji, M., Schofield, C. J., Maxwell, P. H., Pugh, C. W., and Ratcliffe, P. J. (2001) *Science* **292,** 468–472
13. Qi, H. H., Ongusaha, P. P., Myllyharju, J., Cheng, D., Pakkanen, O., Shi, Y., Lee, S. W., and Peng, J. (2008) *Nature* **455,** 421–424
14. Henschen, A. H., Theodor, I., and Pirkle, H. (1991) *Thrombosis Haemostasis* **65,** 821
15. Honda, K., Hayashida, Y., Umaki, T., Okusaka, T., Kosuge, T., Kikuchi, S., Endo, M., Tsuchida, A., Aoki, T., Itoi, T., Moriyasu, F., Hirohashi, S., and Yamada, T. (2005) *Cancer Res.* **65,** 10613–10622
16. Shitashige, M., Satow, R., Honda, K., Ono, M., Hirohashi, S., and Yamada, T. (2008) *Gastroenterology* **134,** 1961–1971, 1971.e1–4
17. Huang, L., Shitashige, M., Satow, R., Honda, K., Ono, M., Yun, J., Tomida, A., Tsuruo, T., Hirohashi, S., and Yamada, T. (2007) *Gastroenterology* **133,** 1569–1578
18. Sakaguchi, N., Kimura, T., Matsushita, S., Fujimura, S., Shibata, J., Araki, M., Sakamoto, T., Minoda, C., and Kuwahara, K. (2005) *J. Immunol.* **174,** 4485–4494
19. Harlow, E., and Lane, D. (1988) *Antibodies. A Laboratory Manual,* Cold Spring Harbor Laboratory, Cold Spring Harbor, NY
20. Sato, S., Idogawa, M., Honda, K., Fujii, G., Kawashima, H., Takekuma, K., Hoshika, A., Hirohashi, S., and Yamada, T. (2005) *Gastroenterology* **129,** 1225–1236
21. Ogata, S., Muramatsu, T., and Kobata, A. (1975) *J. Biochem.* **78,** 687–696
22. Zhang, H., Yi, E. C., Li, X. J., Mallick, P., Kelly-Spratt, K. S., Masselon, C. D., Camp, D. G., 2nd, Smith, R. D., Kemp, C. J., and Aebersold, R. (2005) *Mol. Cell. Proteomics.* **4,** 144–155
23. Hakomori, S. (1989) *Adv. Cancer Res.* **52,** 257–331
24. Ono, M., and Hakomori, S. (2004) *Glycoconj. J.* **20,** 71–78
25. Kumamoto, K., Mitsuoka, C., Izawa, M., Kimura, N., Otsubo, N., Ishida, H., Kiso, M., Yamada, T., Hirohashi, S., and Kannagi, R. (1998) *Biochem. Biophys. Res. Commun.* **247,** 514–517
26. States, D. J., Omenn, G. S., Blackwell, T. W., Fermin, D., Eng, J., Speicher, D. W., and Hanash, S. M. (2006) *Nat. Biotechnol.* **24,** 333–338
27. Kuwahara, K., Yoshida, M., Kondo, E., Sakata, A., Watanabe, Y., Abe, E., Kouno, Y., Tomiyasu, S., Fujimura, S., Tokuhisa, T., Kimura, H., Ezaki, T., and Sakaguchi, N. (2000) *Blood* **95,** 2321–2328
28. Myllyharju, J. (2003) *Matrix Biol.* **22,** 15–24
29. Kukkola, L., Hieta, R., Kivirikko, K. I., and Myllyharju, J. (2003) *J. Biol. Chem.* **278,** 47685–47693
30. Myllyharju, J., and Kivirikko, K. I. (1999) *EMBO J.* **18,** 306–312
31. Gao, J., Opiteck, G. J., Friedrichs, M. S., Dongre, A. R., and Hefta, S. A. (2003) *J. Proteome. Res.* **2,** 643–649
32. Liu, H., Sadygov, R. G., and Yates, J. R., 3rd (2004) *Anal. Chem.* **76,** 4193–4201
33. Ishihama, Y., Oda, Y., Tabata, T., Sato, T., Nagasu, T., Rappsilber, J., and Mann, M. (2005) *Mol. Cell Proteomics.* **4,** 1265–1272
34. Mueller, L. N., Brusniak, M. Y., Mani, D. R., and Aebersold, R. (2008) *J. Proteome. Res.* **7,** 51–61

LEGENDS for SUPPLEMENTARY FIGURES and TABLES

Supplementary Figure S1 and S2 | MS peaks whose intensity was significantly different between pancreatic cancer patients and controls.

Distribution of the intensity of the 6 MS peaks of 412 m/z (RT, 13.7 min), 546 m/z (8.3 min), 552 m/z (8.3 min), 827 m/z (8.3 min), 1141 m/z (29.0 min) and 1185 m/z (9.2 min) in Set 1 (18 pancreatic cancer patients and 19 controls), Set 2 (20 pancreatic cancer patients and 20 controls) and Set 3 (5 pancreatic cancer patients and 4 controls). Lines indicate the mean and standard deviations

Supplementary Figure S3 | MS/MS analysis of the 827-m/z (8.3 min) peak.

Supplementary Figure S4 | MS/MS analysis of the 1141-m/z (29.0 min) peak.

Supplementary Figure S5 | Prolyl 4-hydroxylation of α-fibrinogen.

(A) Amino acid sequence of fibrinogen α -polypeptide isoform α -E preproprotein (NP_000499/NP_068657). Peptides detected by 2DICAL are highlighted in BLUE and 4-hydroxylated proline residues are highlighted in RED.

(B) Chemical structure of 4-hydroxyproline.

Supplementary Figure S6 | Detection of prolyl 4-hydroxylated α-fibrinogen.

(A) Reactivity and titer of 11A5 monoclonal antibody to ESSSHHP(O)GIAEFPSR [P(O), 4-hydroxyproline] peptide (named HyP-ESS) and to unmodified ESSSHHPGIAEFPSR (ESS) peptide determined by antibody capture assay.

(B and C) Plasma αFG-565Hyp and α-fibrinogen levels of healthy controls (C) and pancreatic cancer patients (P) determined by immunoblotting (b) and their correlation (c).

(D) Representative result of competitive ELISA. Serially diluted (10, 5, 2.5, 1.25, 0.63, 0.31, 0.16 and 0.08 μg/ml) standard HyP-ESS peptide (Standard) and plasma samples from 12 pancreatic cancer patients and 12 healthy controls were analysed in triplicate. Note that almost all the samples from pancreatic cancer patients completely inhibited antibody binding.

Supplementary Figure S7

(A) SiRNA suppression measured by RTPCR

(B) The relationship between intensities measured by Western blot densitometry, ELISA and 2DICAL. The horizontal line indicates the intensity of 827 m/z measured by 2DICAL, whereas the vertical lines indicate the Western blot intensity measured by densitometry (left) and ELISA (right) using the 11A5 antibody in the same 22 cases of plasma.

(C) The relationship between 827-m/z and 1141-m/z peak intensities measured by 2DICAL. The horizontal line indicates the intensity of 827 m/z and the vertical line indicates the 1141 m/z intensity in the same 22 cases.

Supplementary Table S1 | Intensity of peptide peaks that were significantly different between the pancreatic cancer patients and healthy controls.

Supplementary Table S2 | Plasma level of αFG-565Hyp in pancreatic cancer patients with different stages.

Supplementary Table S3 | Plasma level of αFG-565Hyp in patients with different diseases.

Supplementary Figure S1

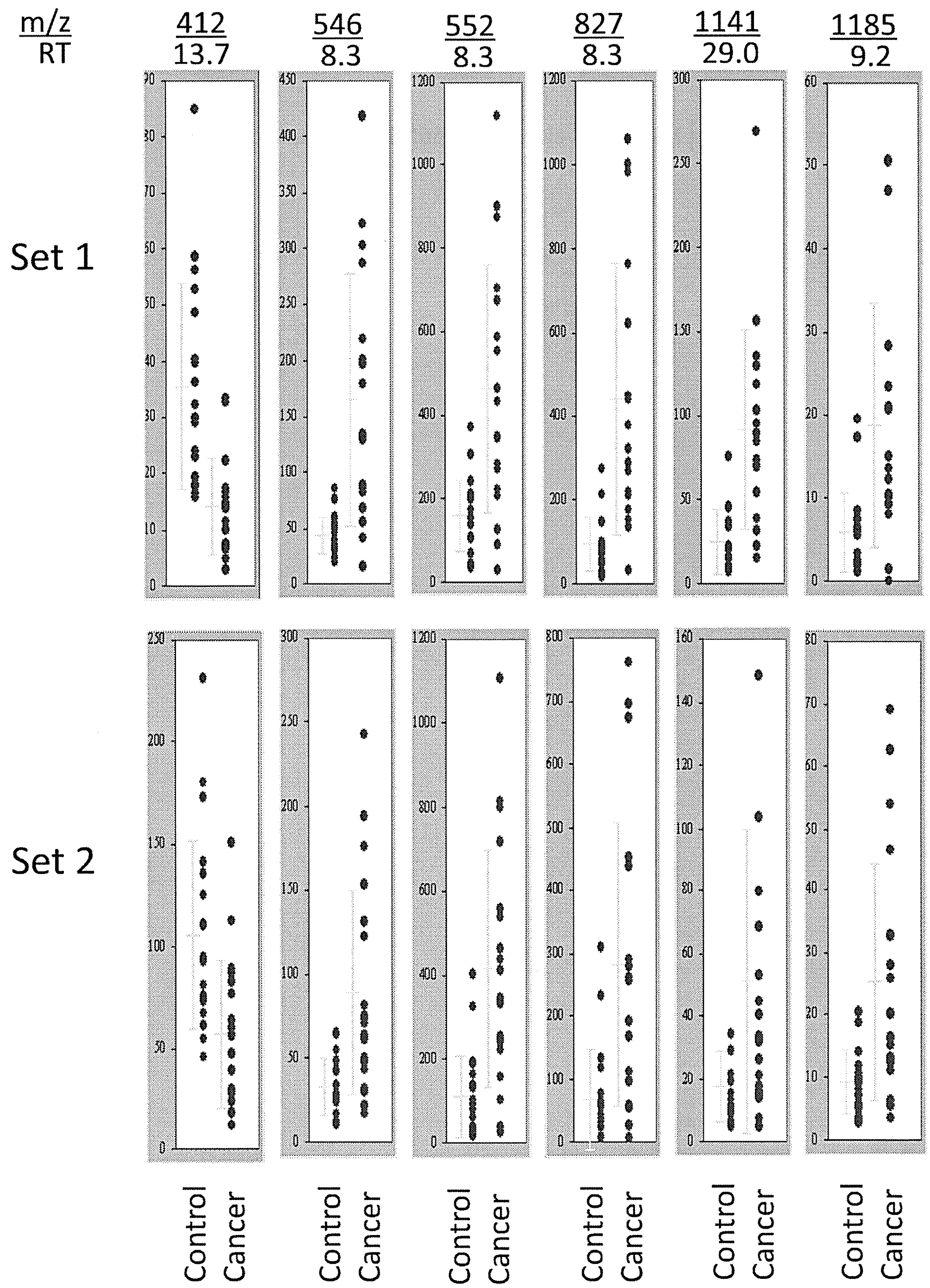

Supplementary Figure S1.
MS peaks whose intensity was significantly different between the pancreatic cancer patients and controls.
Distribution of intensity of the 6 MS peaks in Sets 1 and 2.

Supplementary Figure S2

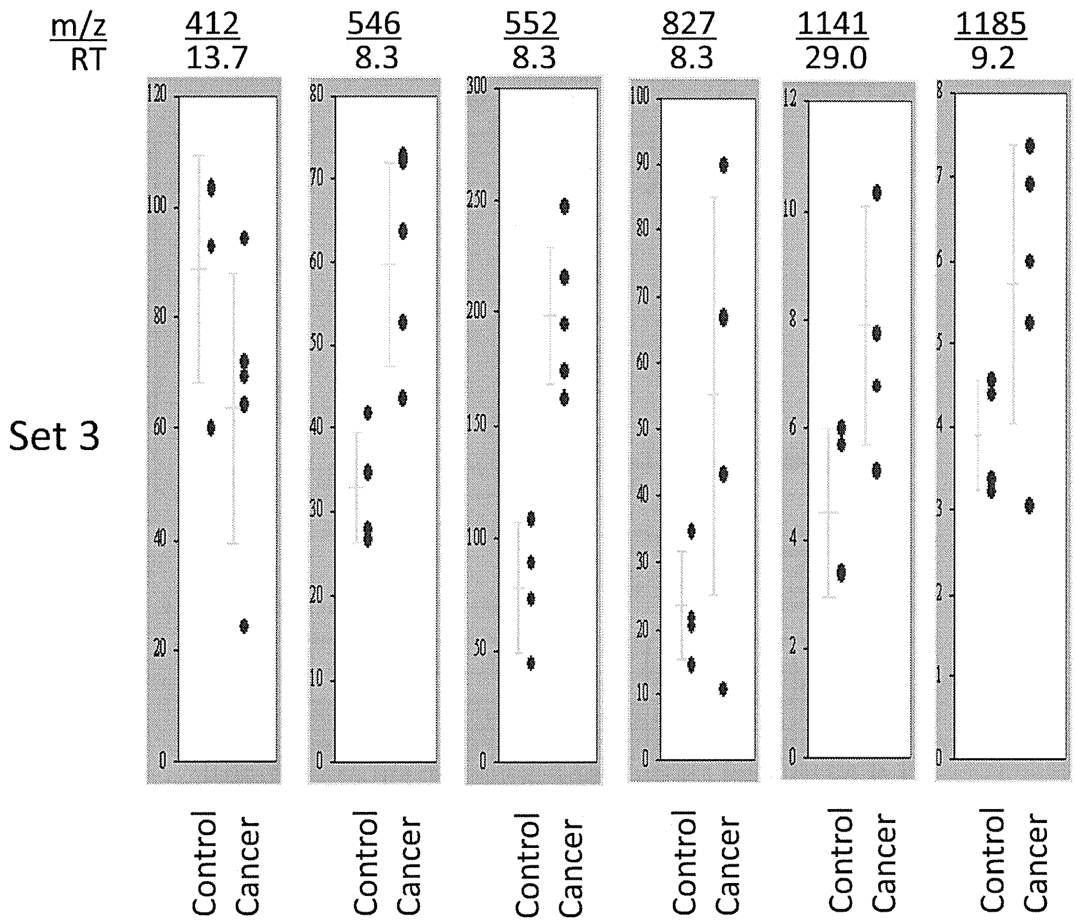

Supplementary Figure S2.
MS peaks whose intensity was significantly different between the pancreatic cancer patients and controls.
Distribution of intensity of the 6 MS peaks in Set 3.

Supplementary Figure S3

Peptide View

MS/MS Fragmentation of ESSSHHPGIAEFPSR
Found in gi|182424, alpha-fibrinogen precursor

Match to Query 117: 1652.623754 from(827.319153,2+)
43977
From data file \\192.168.50.11\fs_project\2dical\Clinical Data\Pancreas
\search\082506C25-10-04-05-01\pkl\43977.txt

Or, Plot from 100 to 1500 Da

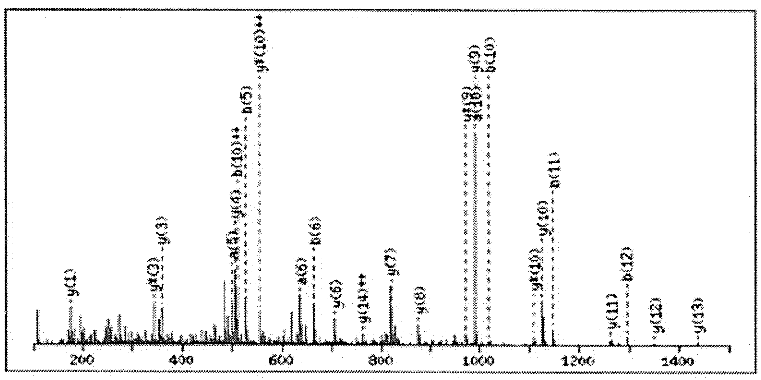

Monoisotopic mass of neutral peptide Mr(calc): 1652.75
Variable modifications:
P7 : Hydroxylation (P)
Ions Score: 65 **Expect:** 0.00039
Matches (Bold Red)**:** 25/112 fragment ions using 58 most intense peaks

#	a	a++	b	b++	Seq.	y	y++	y*	y*++	#
1	102.05	51.53	130.05	65.53	E					15
2	189.09	95.05	217.08	109.04	S	1524.72	762.86	1507.69	754.35	14
3	276.12	138.56	304.11	152.56	S	1437.69	719.35	1420.66	710.83	13
4	363.15	182.08	391.15	196.08	S	1350.65	675.83	1333.63	667.32	12
5	500.21	250.61	528.20	264.61	H	1263.62	632.32	1246.60	623.80	11
6	637.27	319.14	665.26	333.14	H	1126.56	563.79	1109.54	555.27	10
7	750.32	375.66	778.31	389.66	P	989.51	495.26	972.48	486.74	9
8	807.34	404.17	835.33	418.17	G	876.46	438.73	859.43	430.22	8
9	920.42	460.71	948.42	474.71	I	819.44	410.22	802.41	401.71	7
10	991.46	496.23	1019.45	510.23	A	706.35	353.68	689.33	345.17	6
11	1120.50	560.75	1148.50	574.75	E	635.31	318.16	618.29	309.65	5
12	1267.57	634.29	1295.57	648.29	F	506.27	253.64	489.25	245.13	4
13	1364.62	682.82	1392.62	696.81	P	359.20	180.11	342.18	171.59	3
14	1451.65	726.33	1479.65	740.33	S	262.15	131.58	245.12	123.07	2
15					R	175.12	88.06	158.09	79.55	1

Supplementary Figure S3.
MS/MS spectrum of the peptide at 827 m/z and 8.3 min.

Peptide View

MS/MS Fragmentation of TFPGFFSPMLGEFVSETESR
Found in gi|182424, alpha-fibrinogen precursor

Match to Query 269: 2280.895116 from(1141.454834,2+)
83677
From data file \\192.168.50.11\fs_project\2dical\Clinical Data\Pancreas
\search\082506C25-10-04-05-01\pkl\83677.txt

Or, Plot from 100 to 1600 Da

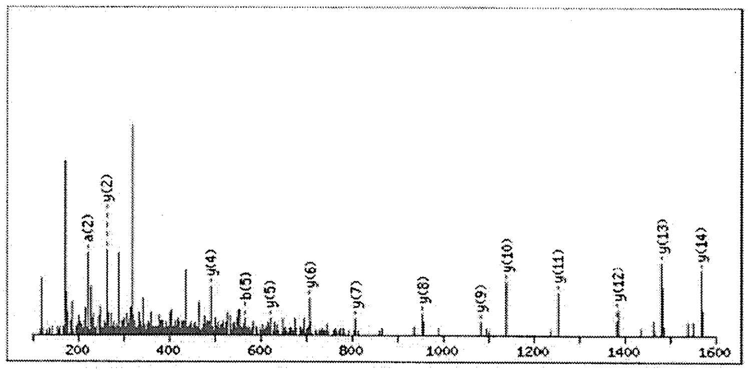

Monoisotopic mass of neutral peptide Mr(calc): 2280.04
Variable modifications:
P3 : Hydroxylation (P)
Ions Score: 65 **Expect:** 0.00039
Matches (Bold Red): 14/152 fragment ions using 39 most intense peaks

#	a	a++	b	b++	Seq.	y	y++	y*	y*++	#
1	74.06	37.53	102.05	51.53	T					20
2	221.13	111.07	249.12	125.07	F	2180.00	1090.50	2162.97	1081.99	19
3	334.18	167.59	362.17	181.59	P	2032.93	1016.97	2015.91	1008.46	18
4	391.20	196.10	419.19	210.10	G	1919.88	960.45	1902.86	951.93	17
5	538.27	269.64	566.26	283.63	F	1862.86	931.94	1845.84	923.42	16
6	685.33	343.17	713.33	357.17	F	1715.79	858.40	1698.77	849.89	15
7	772.37	386.69	800.36	400.68	S	1568.73	784.87	1551.70	776.35	14
8	869.42	435.21	897.41	449.21	P	1481.69	741.35	1464.67	732.84	13
9	1000.46	500.73	1028.45	514.73	M	1384.64	692.82	1367.61	684.31	12
10	1113.54	557.28	1141.54	571.27	L	1253.60	627.30	1236.57	618.79	11
11	1170.57	585.79	1198.56	599.78	G	1140.52	570.76	1123.49	562.25	10
12	1299.61	650.31	1327.60	664.30	E	1083.50	542.25	1066.47	533.74	9
13	1446.68	723.84	1474.67	737.84	F	954.45	477.73	937.43	469.22	8
14	1545.74	773.38	1573.74	787.37	V	807.38	404.20	790.36	395.68	7
15	1632.78	816.89	1660.77	830.89	S	708.32	354.66	691.29	346.15	6
16	1761.82	881.41	1789.81	895.41	E	621.28	311.15	604.26	302.63	5
17	1862.87	931.94	1890.86	945.93	T	492.24	246.62	475.21	238.11	4
18	1991.91	996.46	2019.90	1010.46	E	391.19	196.10	374.17	187.59	3
19	2078.94	1039.97	2106.94	1053.97	S	262.15	131.58	245.12	123.07	2
20					R	175.12	88.06	158.09	79.55	1

Supplementary Figure S4.
MS/MS spectrum of the peptide at 1141 m/z and 29.0 min.